RSC Advances

PAPER

View Article Online
View Journal | View Issue

Cite this: *RSC Adv.*, 2017, **7**, 24368

N-Methylpyrrolidinium hydrogen tartrate (NMPHT): an above-room-temperature order–disorder molecular switchable dielectric material†

Aurang Zeb,[ab] Tariq Khan,[ab] Muhammad Adnan Asghar,[ab] Zhihua Sun,*[a] Zhenyue Wu,[ab] Sangen Zhao[a] and Junhua Luo *[a]

Received 16th January 2017
Accepted 3rd April 2017

DOI: 10.1039/c7ra00689f

rsc.li/rsc-advances

A novel molecular switchable dielectric material *N*-methylpyrrolidinium hydrogen tartrate (**NMPHT**) has been synthesized, which undergoes above room temperature phase transition. Thermal measurements, *e.g.* differential scanning calorimetry and specific heat, confirm the presence of a phase transition around 317.5 K. The dielectric measurement displays a distinct step-like anomaly around T_c, showing two different dielectric states, which reveals that **NMPHT** is a switchable dielectric material. The single-crystal X-ray diffraction analyses at variable temperatures demonstrate that the phase transition emerges from the severe disordering of the *N*-methylpyrrolidinium (NMP) cation, and during the transition the symmetry of **NMPHT** is transformed from higher ($C2/c$) to lower ($P2_1/n$). These findings will provide a new horizon to design smart dielectric structural phase transition materials by incorporating a flexible NMP based scaffold.

1. Introduction

Stimuli-responsive materials are those substances which have the ability to undergo a significant change in their properties under the influence of external stimuli, such as light, radiation, temperature, external pressure, magnetic or electric field, specific chemicals, and pH.[1–10] The architecture and design of such stimuli-responsive structural phase-transition materials (SPTMs) are not only imperative for finding multifunctional materials with novel properties but also very valuable for studying the structure–property relationships.[11–15] Such materials are capable of switching between two or more states, which can thus be employed for multiple purposes[16] including rewritable data storage,[17–20] memory devices,[21–23] switchable dielectric, magnetic and optical functionalities.[24] Generally, these physical responses undergo abrupt changes around the phase transition temperature (T_c).[25] Recently, intensive efforts and strategies have been made to construct switchable dielectric SPTMs in which some physical properties like dielectric constant can be switched between low and high dielectric states around T_c. Among the reported strategies, the most efficient one is to scale-up a single-molecular system exhibiting distinguishable molecular motion, which can be order-disorder transformation, reorientational and rotational motion associated with phase transitions of such materials.[26–30]

It has been experimentally found that the order–disorder transformation of cation affords the driving force for phase transition of the switchable dielectric materials.[29–41] For example, Xiong *et al.* have reported an amphidynamic crystal of $[Me_2NH_2]_2[KCo(CN)_6]$, where the tunable and high dielectric constant is microscopically associated with the order–disorder transformation of $Me_2NH_2^+$ cation.[31]

Likewise, previously several other SPTMs have been reported, conversely, their low T_c restricts their potential device uses.[42–45] In comparison to low temperature, the popular range of T_c is 290–365 K,[46,47] covering around the room temperature range, and they possess widely wonderful applications including pyroelectric sensor, solar, medical, energy-saving and electronic application.[48–55] For example, various salts of glycine molecule with inorganic counterions were discovered to exhibit promising ferroelectricity and pyroelectricity at ambient-temperature.[52,55] Recently we have synthesized a lead-free semiconducting hybrid ferroelectric (*N*-methylpyrrolidinium)$_3$(Sb_2Br_9) in which disordering of *N*-methylpyrrolidinium cation plays key role in temperature trigger phase transition.[56] This work suggests to choose flexible cyclic or acyclic organic amines in order to discover multifunctional SPTM. Therefore, the primitive scaffold pyrrolidinium was selected as promising candidate for designing of such materials.

[a]*State Key Laboratory of Structural Chemistry, Fujian Institute of Research on the Structure of Matter, Chinese Academy of Sciences, Fuzhou, Fujian, 350002, P. R. China. E-mail: jhluo@fjirsm.ac.cn*

[b]*University of the Chinese Academy of Sciences, Beijing 100039, P. R. China. E-mail: sunzhihua@fjirsm.ac.cn*

† Electronic supplementary information (ESI) available: CIF files, PXRD and IR Spectra, DSC at different scanning rates, TG/DTA curves, crystal packing diagrams, thermal ellipsoidal view of cation–anion, temperature-dependent cycle of dielectric constant at 1 MHz, table of crystal data, entropy change calculations. CCDC reference numbers 1521921 and 1521922 for **NMPHT** at 260 K, and 330 K. For ESI and crystallographic data in CIF or other electronic format see DOI: 10.1039/c7ra00689f

As a continuous study of order–disorder systems in SPTMs,[37–41] the disordered *N*-methylpyrrolidinium (NMP) cation has been incorporated to assemble a new phase transition compound, *N*-methylpyrrolidinium hydrogen tartrate (**NMPHT**), which undergoes a reversible phase transition at 317.5 K in dielectric measurement. The phase transition of **NMPHT** has been confirmed through thermal analyses, such as, differential scanning calorimetry (DSC) and heat capacity (C_P). The variable temperature single-crystal X-ray diffraction (SCXRD) analyses reveal that the order-disorder transformation of flexible *N*-methylpyrrolidinium cation is the driving force for phase transition in **NMPHT**. Importantly the structurally flexible, pyrrolidinium based scaffold easily undergo order–disorder transformation or reorient at above room temperature. This finding might be helpful to design smart SPTMs of promising dielectric properties.

2. Experimental

2.1 Synthesis

All the reagents and solvents were used of analytical grade without further purification, unless otherwise stated. Equivalent molar, *N*-methylpyrrolidine (2 mL, 0.002 mol) and tartaric acid (3 g, 0.002 mol) were dissolved in 40 mL of distilled water and was stirred for 2 h. The crystals of **NMPHT** were obtained after two weeks by slow evaporation at room temperature. The purity of bulk material of **NMPHT** was checked by powder X-ray diffraction (PXRD). The recorded diffraction patterns were significantly matchable with the pattern simulated from the single-crystal X-ray diffraction (SCXRD) structure of **NMPHT** (Fig. S1†).

2.2 Dielectric measurements

The well-ground powder samples with silver-conducting paste were used for dielectric studies. The complex dielectric permittivity ε ($\varepsilon = \varepsilon' - i\varepsilon''$) were measured using a TH2828A impedance analyzer over the frequency range of 500 kHz to 1 MHz, and in the temperature range from 290 K to 360 K. The measuring AC voltage fixed at 1 V.

2.3 Thermal measurements

Differential scanning calorimetry (DSC) was carried out on a NETZCSCH DSC 200 F3 instrument at rate of 2 K min^{-1}, 5 K min^{-1} and 10 K min^{-1} for both heating as well as cooling mode in the temperature range 280–360 K (Fig. S3†). These measurements were performed at atmospheric pressure under nitrogen environment in aluminum crucibles. In addition to DSC, specific heat (C_P) experiments were also performed for which sapphire standard was used as a reference.

2.4 Powder X-ray diffraction (PXRD) and IR spectra

MiniFlex II Powder X-Ray Diffractometer was used to confirm the phase purity of **NMPHT** by recording powder X-ray diffraction (PXRD) pattern at room temperature in the 2θ range of 5–45° (Fig. S1†). IR spectrum was recorded on VERTEX 70 Infrared Spectrometer, which displayed several vibrations around 1710 cm^{-1}($\bar{\nu}_{COOH}$) for COOH group, 1600 cm^{-1} for asymmetric and 1400 cm^{-1} for symmetric stretches of carboxylate group of tartrate anion. While the peak around 3000 cm^{-1}($\bar{\nu}_{C-H}$) and 2700 cm^{-1} ($\bar{\nu}_{R3NH^+}$) are due to stretching vibration absorption of the C–H sp^3 carbon atom and protonated N atom of NMP cation which confirming the formation of **NMPHT** (Fig. S2†).

2.5 Single crystal structure determination

The variable-temperature single-crystal X-ray diffraction (SCXRD) data of synthesized sample were obtained from a Rigaku CCD (charge-coupled device) diffractometer with Cu-Kα radiation of wavelength (λ) '1.54184 Å' at variable-temperature that is, at 260 K and 330 K as low and high temperatures respectively. Crystal structures of **NMPHT** were solved by direct methods while refinement was carried out by full-matrix least-squares method based on F^2 using the SHELXLTL software package.[57] All non-hydrogen (non-H) atoms were anisotropically refined. The positions of H atoms of NMP cation and tartrate anion were geometrically generated. Table S1,† gives the detailed description of the crystallographic data, as well as data collection and refinement at 260 K and 330 K. The R_1 factors, in the SCXRD for **NMPHT**, were found to be slightly large. This is because the crystal data collections of **NMPHT** were carried out at ambient temperature. The Cambridge Crystallographic Data Centre (CCDC) 1521921–1521922 for **NMPHT** contains the supplementary crystallographic data for this paper.

3. Results and discussion

3.1 Thermal properties

DSC measurement is usually applied as a primary tool to investigate phase transition in thermo-responsive materials.[37–41] In **NMPHT** the endothermic and exothermic reversible anomalies appear at 317.5 and 312.2 K, respectively, which confirms the occurrence of a reversible phase transition as shown in Fig. 1a. The sharp-shaped of the observed anomalies and the large value of heat hysteresis ~5.3 K indicates a typical first-order phase transition.[39–42] It is interesting that the T_c of **NMPHT** is not only higher than room temperature, but much lower than the melting point (403 K) as well as decomposition (~540 K) (as demonstrated in the TG/DTA curves, Fig. S4†). Such temperature interval shows the significant thermal stability of the title compound, which will greatly facilitate its potential application.

Furthermore, the phase transition in **NMPHT** was also confirmed by C_P experiments as given in Fig. 1b. The C_P curve in C_P–T graph displays a sharp peak at phase transition temperature (T_c), which matches very well with the DSC result. The enthalpy change (ΔH) is measured as 2311.9 J mol^{-1} while entropy change (ΔS), calculated by calculus methods, is 7.281 J mol^{-1} K^{-1} on the heating process (calculation has been given at the end of ESI†). According to Boltzmann's equation, $\Delta S = R \ln N$, where R is the universal gas constant and N is the ratio of possible orientations. The value of N is estimated as 2.40 which clearly suggests an order-disorder behavior in **NMPHT**.[42,43]

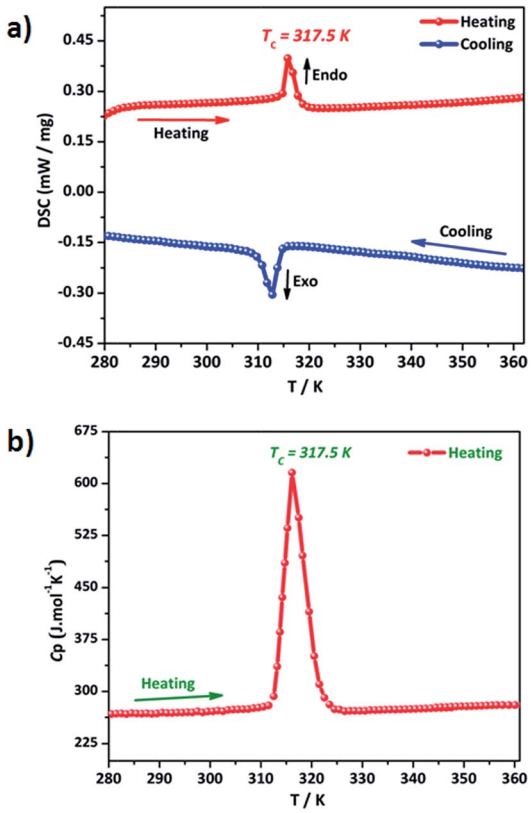

Fig. 1 (a) Reversible DSC curves, and (b) C_P of **NMPHT**.

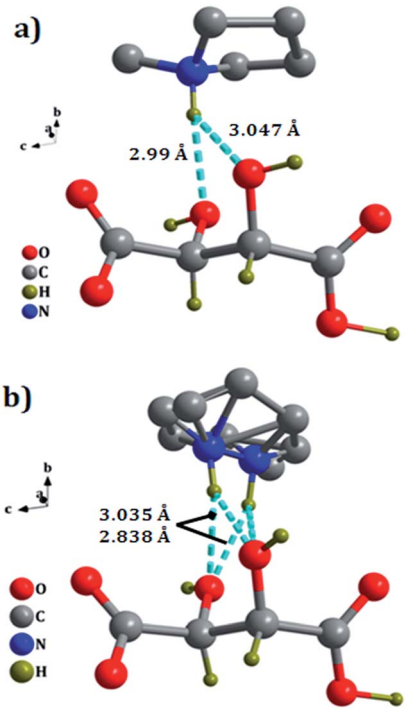

Fig. 2 The asymmetric unit of **NMPHT** (a) at LTP (b) at HTP. Carbon-bonded H-atoms of NMP cation are omitted for clarity.

3.2 Single crystal structure determination

The SCXRD structural analyses of **NMPHT** were performed at 260 K (LTP, low-temperature phase) and 330 K (HTP, high-temperature phase). In both phases, **NMPHT** crystallizes in the same monoclinic crystal system with different centrosymmetric space group, *i.e.*, $P2_1/n$ and $C2/c$, at LTP and HTP, respectively. The cell parameters for HTP are $a = 11.7014(5)$ Å, $b = 8.7644(3)$ Å, $c = 12.0457(3)$ Å, $\alpha = \gamma = 90°$, $\beta = 107.298(4)°$, $V = 1179.48(7)$ Å^3 and $Z = 4$, while for LTP, the cell parameters are $a = 11.3346(4)$ Å, $b = 8.7794(3)$ Å, $c = 12.0991(4)$ Å, $\alpha = \gamma = 90°$, $\beta = 106.683(4)°$, $V = 1153.31(7)$ Å^3, and $Z = 4$ as given in the Table S1.†

The asymmetric unit of **NMPHT** in the LTP contains one protonated NMP cation and one monodeprotonated tartrate $[(C_4H_5O_6)^-]$ anion. In the HTP, the asymmetric unit becomes half and it includes one-half of cation and anion each (Fig. 2). As provided in Fig. 3, it is clear that in the HTP, the cation is highly disordered and its disordered atoms reside over two sites. In detail, the cyclic aliphatic part including the nitrogen atom, as well as carbon atom of methyl group of the NMP cation show prominently disorder behavior. The NMP is sternly disordered, where NA/NB, C1A/C1B, C3A/C3B and C4A/C4B atoms are located over two positions, as illustrated in the Fig. 3b. The occupancy factor of NA/NB, C1A/C1B, C3A/C3B and C4A/C4B of NMP, is 0.5 : 0.5 for each disordered atom, which clearly demonstrates that all disordered states are in equivalent distribution. Above T_c, the distinctive thermal ellipsoidal behavior of these atoms of cation is greater than the neighboring atoms. Certainly, this is not the actual state, but an average result for the disordering of atoms which discloses that the cation undergoes into highly disordered state (Fig. S6b†). The disordered state of these atoms is accomplished by splitting of each atom into two different positions. Below T_c, with the lowering of temperature, the disordering of cation is ceased and it results into a completely ordered state. Thus, the crystal structure of the dynamically frozen NMP below T_c corresponds to more stabilized state, as has been shown in Fig. S6a.† Therefore, the thermal splitting of the nitrogen and carbon atoms in cation assures the possible flexible nature of NMP scaffold.

The SCXRD analyses reveal that in the packing structures of **NMPHT**, there exists a network of hydrogen bonding at both LTP and HTP. These interactions have been observed among

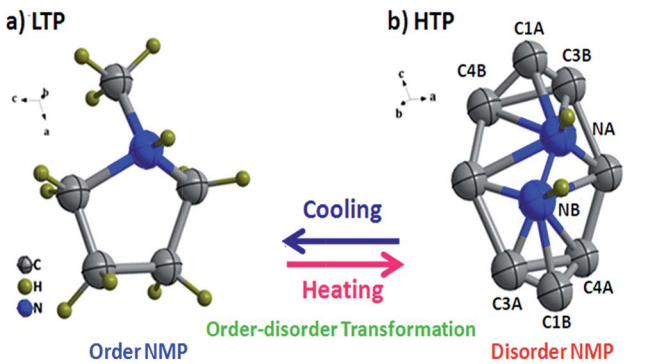

Fig. 3 Order–disorder transformation of NMP cation in **NMPHT** during phase transition. The cation (a) in order state at LTP, and (b) in disordered state at HTP.

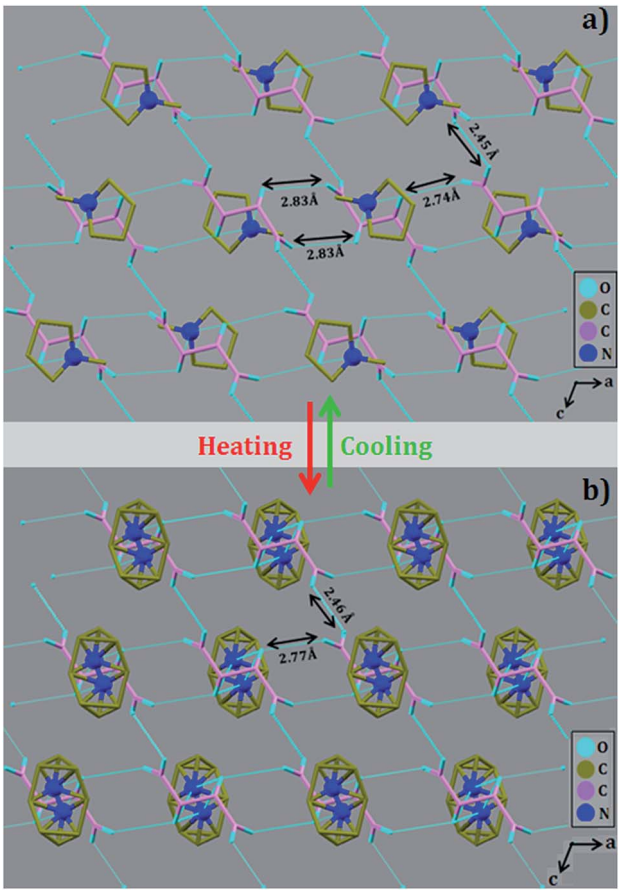

Fig. 4 The packing diagram of **NMPHT**, showing both anion–anion and anion–cation hydrogen bonding at (a) LTP, and (b) HTP.

the anion–anion and anion–cation, as shown in Fig. S5.† The adjacent tartrate anions are connected through the carboxylic groups *via* O–H···O, as can be viewed from the direction of *b*-axis (Fig. 4). The resultant one dimensional parallel anionic chains are linked sidewise to each other through hydrogen bond (O–H···O), which exists between the hydroxyl group of one anion and the carbonyl oxygen of another. The overall hydrogen bonding makes two dimensional skeletons, which extend in the direction of *a*- and *b*-axis (Fig. 4). The anion–cation interactions (N–H···O) are between the nitrogen atom of NMP cation and hydroxyl oxygen (OH) of anion. However, there are ignorable differences found in the hydrogen bonding between LTP and HTP in **NMPHT**.

The analysis based on the symmetry transformation viewpoint of **NMPHT** shows that during phase transition the symmetry change occurs from the high centrosymmetric space group $C2/c$ with point group C_{2h}^{6} at HTP to the low centrosymmetric space group $P2_1/n$ with point group C_{2h}^{5} at LTP.[58,59] During the phase transition the symmetric elements (E, C_2, i, σ_h) remains unchanged at both phases (Fig. 5). The symmetry transformation from HTP to LTP clearly demonstrates the lack of group–subgroup relationship based on the Curie symmetry principle.[37,59–61]

From above discussion this can be concluded that the structural phase transition in **NMPHT** is attributed to the severe

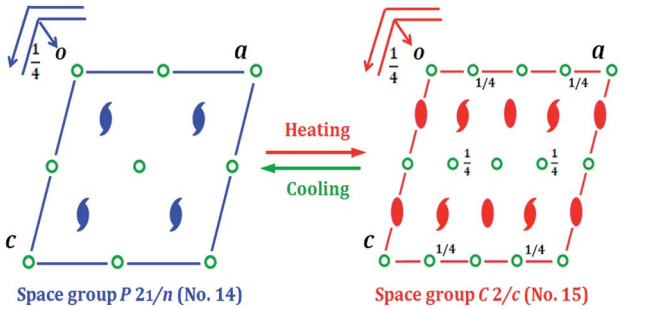

Fig. 5 Symmetry transformation of space group in **NMPHT** from the $P2_1/n$ (LTP) to a $C2/c$ (HTP).

disordering of NMP cation. The detail SCXRD studies reveal that at HTP, the cyclic aliphatic moiety including the nitrogen along with the methyl group of NMP cation are disordered. As temperature decreases below T_c, the disordering of cation is frozen and it transforms into completely ordered state. During transition from above to below T_c, symmetry transformation occurs from higher ($C2/c$) to lower ($P2_1/n$). We believe that these findings will provide a new route to design smart dielectric SPTMs by incorporating flexible NMP.

3.3 Dielectric studies of NMPHT

Temperature dependent dielectric constant is a significant tool to measure the dielectric response in thermally induced SPTMs.[39–42,62,63] In molecular crystals, the disordering behavior or reorientation contributes a major part to the dielectric switching.[62–64] For **NMPHT** the well-ground powder-pressed sample with silver-conducting paste was used to perform temperature-dependent dielectric experiments. The complex dielectric permittivity ε ($\varepsilon = \varepsilon' - i\varepsilon''$, where ε' and ε'' are the real and imaginary parts, respectively) was measured at 500 kHz and 1 MHz frequencies in the temperature range of 290–360 K as given in Fig. 6. The step-shaped dielectric

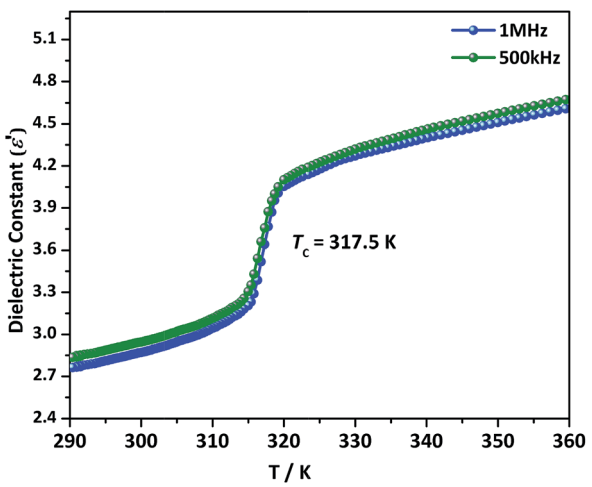

Fig. 6 Temperature dependent dielectric constants of **NMPHT** carried out on the powder pressed pellets at 500 kHz and 1 MHz frequencies during heating mode.

anomaly was clearly observed at 317.5 K during the endothermic part of thermal process, which clearly reveals the existence of the phase transition in **NMPHT**. The results obtained from dielectric measurement are well-matched with that of DSC and C_P measurements. The ε' value increases gradually until 315 K and subsequently it displays a noticeable step-like increment around T_c. The ε' value of **NMPHT** swiftly jumps from 3.2 to 4.1 around T_c (Fig. 6). The temperature-triggered step-like dielectric anomalies in the vicinity of T_c is the characteristic feature of switchable dielectric materials,[63,64] and existence of order–disorder transformation.[62,64] In the Fig. S7,† the ε' displays two step-like dielectric anomalies in the heating (at 317.5 K) and cooling (at 312.2 K) processes, consistent with DSC results. These anomalies exhibited the reversible dielectric switching between two dielectric states. The switching dielectric behavior observed in the **NMPHT**, was assumed to be because of the order–disorder phenomenon occurring in NMP cation. All these findings lead us to conclude that **NMPHT** might be a potential thermo-responsive switchable dielectric molecular material.

4. Conclusions

In this work, we report an above-room-temperature molecular switchable dielectric material exhibiting a reversible phase transition at 317.5 K, which is confirmed by dielectric measurements, thermal and single crystal X-ray diffraction analyses. The phase transition in **NMPHT** is mainly originated from the order–disorder transformation of the NMP cation. In detail, during cooling process, the highly disordered NMP cation is frozen and become fully ordered, which leads to the phase transition in **NMPHT**. This new finding is the continuation of our previous work[56] and suggesting for the selection of flexible NMP based scaffold, which might open up a new route to design potential SPTMs with intriguing properties.

Acknowledgements

A. Zeb is thankful to the CAS-TWAS President program of the UCAS (University of the Chinese Academy of Sciences) for the financial support. This work is financially supported by NSFC (21373220, 21525104, 91422301, 51402296 and 515022910), Youth Innovation Promotion of CAS (2014262) and the State Key Laboratory of Luminescence and Applications (SKLA-2016-09).

Notes and references

1 *Handbook of Stimuli-Responsive Materials*, ed. M. W. Urban, Wiley-VCH, Weinheim, Germany, 2011, pp. 1–278.
2 M. A. C. Stuart, W. T. S. Huck, J. Genzer, M. Müller, C. Ober, M. Stamm, G. B. Sukhorukov, I. Szleifer, V. V. Tsukruk, M. Urban, F. Winnik, S. Zauscher, I. Luzinov and S. Minko, *Nat. Mater.*, 2010, **9**, 101–113.
3 S. Horike, S. Shimomura and S. Kitagawa, *Nat. Chem.*, 2009, **1**, 695–704.
4 W. Zhang and R.-G. Xiong, *Chem. Rev.*, 2012, **112**, 1163–1195.
5 O. Sato, J. Tao and Y.-Z. Zhang, *Angew. Chem., Int. Ed.*, 2007, **46**, 2152–2187.
6 Z.-Y. Du, T.-T. Xu, B. Huang, Y.-J. Su, W. Xue, C.-T. He, W.-X. Zhang and X.-M. Chen, *Angew. Chem., Int. Ed.*, 2015, **54**, 914–918.
7 C. Shi, X. Zhang, Y. Cai, Y.-F. Yao and W. Zhang, *Angew. Chem., Int. Ed.*, 2015, **54**, 6206–6210.
8 W.-Q. Liao, H.-Y. Ye, D.-W. Fu, P.-F. Li, L.-Z. Chen and Y. Zhang, *Inorg. Chem.*, 2014, **53**, 11146–11151.
9 A. U. Petersen, M. Jevric, R. J. Mandle, E. J. Davis, S. J. Cowling, J. W. Goodby and M. B. Nielsen, *RSC Adv.*, 2015, **5**, 89731–89744.
10 A. U. Petersen, M. Jevric, R. J. Mandle, M. T. Sims, J. N. Moore, S. J. Cowling, J. W. Goodby and M. B. Nielsen, *Chem.–Eur. J.*, 2017, DOI: 10.1002/chem.201700055.
11 J.-Z. Ge, X.-Q. Fu, T. Hang, Q. Ye and R.-G. Xiong, *Cryst. Growth Des.*, 2010, **10**, 3632–3637.
12 Q. Ye, T. Akutagawa, N. Hoshino, T. Kikuchi, S. Noro, R.-G. Xiong and T. Nakamura, *Cryst. Growth Des.*, 2011, **11**, 4175–4182.
13 Y. Zhang, W.-Q. Liao, H.-Y. Ye, D.-W. Fu and R.-G. Xiong, *Cryst. Growth Des.*, 2013, **13**, 4025–4030.
14 Z. H. Sun, J. H. Luo, T. L. Chen, L. Li, R.-G. Xiong, M.-L. Tong and M. C. Hong, *Adv. Funct. Mater.*, 2012, **22**, 4855–4861.
15 M. A. Asghar, Z. H. Sun, T. Khan, C. M. Ji, S. Q. Zhang, S. Liu, L. Li, S. G. Zhao and J. H. Luo, *Cryst. Growth Des.*, 2016, **16**, 895–899.
16 H. K. Henisch, R. Roy and L. E. Cross, *Phase Transition*, Pergamon Press, New York, 1973.
17 M. Wuttig, *Nat. Mater.*, 2006, **5**, 56–62.
18 M. Wuttig and N. Yamada, *Nat. Mater.*, 2007, **6**, 824–832.
19 D. Lencer, M. Salinga and M. Wuttig, *Adv. Mater.*, 2011, **23**, 2030–2058.
20 K. Uchino, *Ferroelectric Devices*, Marcel Dekker, New York, 2000.
21 J. F. Scott, *Science*, 2007, **315**, 954–959.
22 N. Yamada and T. Matsunaga, *J. Appl. Phys.*, 2000, **88**, 7020–7028.
23 M. Wuttig, *Nat. Mater.*, 2005, **4**, 265–266.
24 P.-P. Shi, Q. Ye, Q. Li, H.-T. Wang, D.-W. Fu, Y. Zhang and R.-G. Xiong, *Chem. Mater.*, 2014, **26**, 6042–6049.
25 M. Fujimoto, *The Physics of Structural Phase Transitions*, Springer, New York, 2005.
26 M. Ptak, M. Mączka, A. Gągor, A. Sieradzki, A. Stroppa, D. D. Sante, J. M. Perez-Mato and L. Macalik, *Dalton Trans.*, 2016, **45**, 2574–2583.
27 P. Zhou, Z. H. Sun, S. Q. Zhang, C. M. Ji, S. G. Zhao, R.-G. Xiong and J. H. Luo, *J. Mater. Chem. C*, 2014, **2**, 2341–2345.
28 S. Zeng, Z. H. Sun, C. M. Ji, S. Q. Zhang, C. Song and J. H. Luo, *CrystEngComm*, 2016, **18**, 3606–3611.
29 Z.-X. Wang, W.-Q. Liao, H.-Y. Ye and Y. Zhang, *Dalton Trans.*, 2015, **44**, 20406–20412.
30 W. Zhang, H.-Y. Ye, R. Graf, H. W. Spiess, Y.-F. Yao, R. Q. Zhu and R.-G. Xiong, *J. Am. Chem. Soc.*, 2013, **135**, 5230–5233.
31 W.-Q. Liao, G.-Q. Mei, H.-Y. Ye, Y.-X. Mei and Y. Zhang, *Inorg. Chem.*, 2014, **53**, 8913–8918.

32 X. Zhang, X.-D. Shao, S.-C. Li, Y. Cai, Y.-F. Yao, R.-G. Xiong and W. Zhang, *Chem. Commun.*, 2015, **51**, 4568–4571.
33 G.-Q. Mei, H.-Y. Zhang and W.-Q. Liao, *Chem. Commun.*, 2016, **52**, 11135–11138.
34 C.-Y. Mao, W.-Q. Liao, Z.-X. Wang, Z. Zafar, P.-F. Li, X.-H. Lv and D.-W. Fu, *Inorg. Chem.*, 2016, **55**, 7661–7666.
35 Y. Zhou, T. L. Chen, Z. H. Sun, S. Q. Zhang, S. G. Zhao, C. M. Ji, C. Song and J. H. Luo, *CrystEngComm*, 2016, **18**, 2852–2856.
36 K. Qian, F. Shao, Z. H. Yan, J. Pang, X. D. Chen and C. X. Yang, *CrystEngComm*, 2016, **18**, 7671–7674.
37 C. M. Ji, Z. H. Sun, S. Q. Zhang, T. L. Chen, P. Zhou and J. H. Luo, *J. Mater. Chem. C*, 2014, **2**, 567–572.
38 Z. H. Sun, X. Q. Wang, J. H. Luo, S. Q. Zhang, D. Q. Yuan and M. C. Hong, *J. Mater. Chem. C*, 2013, **1**, 2561–2567.
39 M. A. Asghar, C. M. Ji, Y. Zhou, Z. H. Sun, T. Khan, S. Q. Zhang, S. G. Zhao and J. H. Luo, *J. Mater. Chem. C*, 2015, **3**, 6053–6057.
40 T. Khan, Y. Y. Tang, Z. H. Sun, S. Q. Zhang, M. A. Asghar, T. L. Chen, S. G. Zhao and J. H. Luo, *Cryst. Growth Des.*, 2015, **15**, 5263–5268.
41 T. Khan, M. A. Asghar, Z. H. Sun, A. Zeb, L. Li, S. Liu, S. G. Zhao, C. M. Ji and J. H. Luo, *Chem.–Asian J.*, 2016, **11**, 2876–2881.
42 M. A. Asghar, S. Q. Zhang, T. Khan, Z. H. Sun, A. Zeb, C. M. Ji, L. Li, S. G. Zhao and J. H. Luo, *J. Mater. Chem. C*, 2016, **4**, 7537–7540.
43 T. Besara, P. Jain, N. S. Dalal, P. L. Kuhns, A. P. Reyes, H. W. Kroto and A. K. Cheetham, *Proc. Natl. Acad. Sci. U. S. A.*, 2011, **108**, 6828–6832.
44 A. Stroppa, P. Barone, P. Jain, J. M. Perez-Mato and S. Picozzi, *Adv. Mater.*, 2013, **25**, 2284–2290.
45 D.-W. Fu, H.-L. Cai, S. H. Li, Q. Ye, L. Zhou, W. Zhang, Y. Zhang, F. Deng and R.-G. Xiong, *Phys. Rev. Lett.*, 2013, **110**, 257601.
46 K. Pielichowska and K. Pielichowski, *Prog. Mater. Sci.*, 2014, **65**, 67–123.
47 S. Benita, *Microencapsulation: Methods and Industrial Applications*, Marcel Dekker, New York, USA, 1996.
48 S.-H. Baek, C. M. Folkman, J.-W. Park, S. Lee, C.-W. Bark, T. Tybell and C.-B. Eom, *Adv. Mater.*, 2011, **23**, 1621–1625.
49 I. Gur, K. Sawyer and R. Prasher, *Science*, 2012, **335**, 1454–1455.
50 A. Sharma, V. V. Tyagi, C. R. Chen and D. Buddhi, *Renewable Sustainable Energy Rev.*, 2009, **13**, 318–345.
51 Y. Zhang, G. Zhou, K. Lin, Q. Zhang and H. Di, *Energy Build.*, 2007, **42**, 2197–2209.
52 S. Horiuchi and Y. Tokura, *Nat. Mater.*, 2008, **7**, 357–366.
53 R. Pepinsky, K. Vedam, S. Hoshino and Y. Okaya, *Phys. Rev.*, 1958, **111**, 430–432.
54 F. Jona and G. Shirane, *Phys. Rev.*, 1960, **117**, 139–142.
55 S. Hoshino, T. Mitsui, F. Jona and R. Pepinsky, *Phys. Rev.*, 1957, **107**, 1255–1258.
56 Z. H. Sun, A. Zeb, S. Liu, C. M. Ji, T. Khan, L. Li, M. C. Hong and J. H. Luo, *Angew. Chem. Int. Ed.*, 2016, **55**, 11854–11858; *Angew. Chem.*, 2016, **128**, 12033–12037.
57 G. M. Sheldrick, *SHELXL-97: Programs for X-ray Crystal Structure Solution*, University of Göttingen, Göttingen, Germany, 1997.
58 *International Tables for Crystallography, Volume A: Space-Group Symmetry*, The International Union of Crystallography, ed. T. Hahn, Springer, 5th edn, 2005.
59 Y. A. Izyumov and V. N. Syromyatnikov, *Phase Transitions and Crystal Symmetry*, Kluwer Academic Publishers, Dordrecht, 1990.
60 I. S. Zhedudev, in *Solid State Phys. Adv. Res. App.*, ed. H. Ehrenreich, F. Seitz and D. Turnbull, Academic Press, New York, 1971, vol. 26, p. 429.
61 P. Zhou, Z. H. Sun, S. Q. Zhang, T. L. Chen, C. M. Ji, S. G. Zhao and J. H. Luo, *Chem.–Asian J.*, 2014, **9**, 996–1000.
62 T. Khan, M. A. Asghar, Z. H. Sun, C. M. Ji, L. Li, S. G. Zhao and J. H. Luo, *RSC Adv.*, 2016, **6**, 69546–69550.
63 H. Fröhlich, *Theory of Dielectrics*, Oxford University Press, Oxford, UK, 1991.
64 X.-D. Shao, X. Zhang, C. Shi, Y.-F. Yao and W. Zhang, *Adv. Sci.*, 2015, **2**, 1500029.